Comparison of the heat transfer characteristics of molten salt, liquid sodium and supercritical CO_2 in bayonet tubes of solar tower receivers

Cite as: AIP Conference Proceedings **2126**, 080005 (2019); https://doi.org/10.1063/1.5117600
Published Online: 26 July 2019

R. Pérez-Álvarez, C. Marugán-Cruz, D. Santana-Santana, and A. Acosta-Iborra

Comparison of the Heat Transfer Characteristics of Molten Salt, Liquid Sodium and Supercritical CO_2 in Bayonet Tubes of Solar Tower Receivers

R. Pérez-Álvarez[1, a)], C. Marugán-Cruz[1], D. Santana-Santana[1], and A. Acosta-Iborra[1]

[1]*Energy Systems Engineering Group (ISE). Department of Thermal and Fluids Engineering, Universidad Carlos III de Madrid. Avda. de la Universidad 30, Leganés 28911, Madrid (Spain).*

[a)]Corresponding author: rafperez @ing.uc3m.es

Abstract. The solar tower receivers tend to experience rupture problems due to the high thermal gradients and the corrosion produced by the working fluid, typically solar salt. In this work we have developed a series of CFD simulations to study a new receiver design composed of bayonet tubes aimed to reduce the overheating the receiver in the most thermally demanded area. These simulations evaluate the thermal behavior of the tubes for different working fluids, i.e. molten salt, liquid sodium and supercritical CO_2.The simulations show that, for all the working fluids analyzed, it is possible to reduce the high temperatures of the tube thanks to the asymmetries created when the bayonet tube has an eccentric configuration. Besides, the greatest reduction of temperature in bayonet tubes is achieved when the working fluid is liquid sodium due to its higher thermal conductivity.

INTRODUCTION

The use of solar energy for the production of electricity is experiencing a significant growth due to the social awareness regarding the environmental protection and the increasing price of fossil fuels. Among the current developments of this type of energy stand out the plants of solar power tower type with thermal storage, because they are capable of achieving high thermal efficiency as well as having a high number of hours of operation. However, in practice, they are far from their full potential of performance owing to operation problems that still have to be solved. One of the main problems is the rupture of the receiver tubes due to the high thermal gradients to which they are subjected and the corrosion caused by the working fluid, which is typically a molten salt. There are different ways to solve these problems. One way is the substitution of the molten salt by another less corrosive working fluid such as liquid sodium or supercritical CO_2 (sCO_2). Another way is the design of a new receiver configurations able to reduce the overheating of the receiver.

In this work a new receiver configuration will be studied. This receiver is composed of bayonet tubes instead of simple tubes, Fig. 1 (a), as proposed in [1]. The working fluid flows first through the circular section of the inner tube and then returns through the annular section of the gap between the inner and outer tubes. The heat absorbed by the outer tube, coming from the solar radiation concentrated by the heliostats of the plant, heats the fluid in the annular section. A fraction of this heat is exchanged between the flow that circulates through the annular section and that of the circular section, which is cooler. This avoids the excessive overheating of the fluid and the walls of the bayonet tube compared to simple tube receivers.

In an eccentric bayonet tube the inner and the outer tubes are not concentric, and their centers are separated by a distance, e. The eccentricity, ξ, of the bayonet tube is defined as follows

SolarPACES 2018
AIP Conf. Proc. 2126, 080005-1–080005-8; https://doi.org/10.1063/1.5117600
Published by AIP Publishing. 978-0-7354-1866-0/$30.00

$$\xi = \frac{e}{D_i - d_e} \tag{1}$$

Where D_i is the inner diameter of the outer tube and d_e is the outer diameter of the inner tube.

The asymmetry of the flow characteristics in a bayonet tube can be used to increase the heat transfer coefficient in the angular direction of the tube where the solar radiation is maximum, $\theta = 0°$ in Fig. 1 (b). This opens up the possibility of further reducing the temperature gradients in the bayonet tubes of solar receivers while slightly decreasing the pressure drop in the annular section. This effect has only been confirmed for molten salt [2]. However, in order to optimize the design of these receivers, it would be advisable to study their behavior for other working fluids.

The aim of the present work is to jointly characterize the effect of the eccentricity, and the type of working fluid (molten salt, liquid sodium or sCO_2) on the heat transfer characteristics of a bayonet tube receiver. This study will focus on the annular section of the bayonet tube, which is the most complex and thermally demanded part of the system.

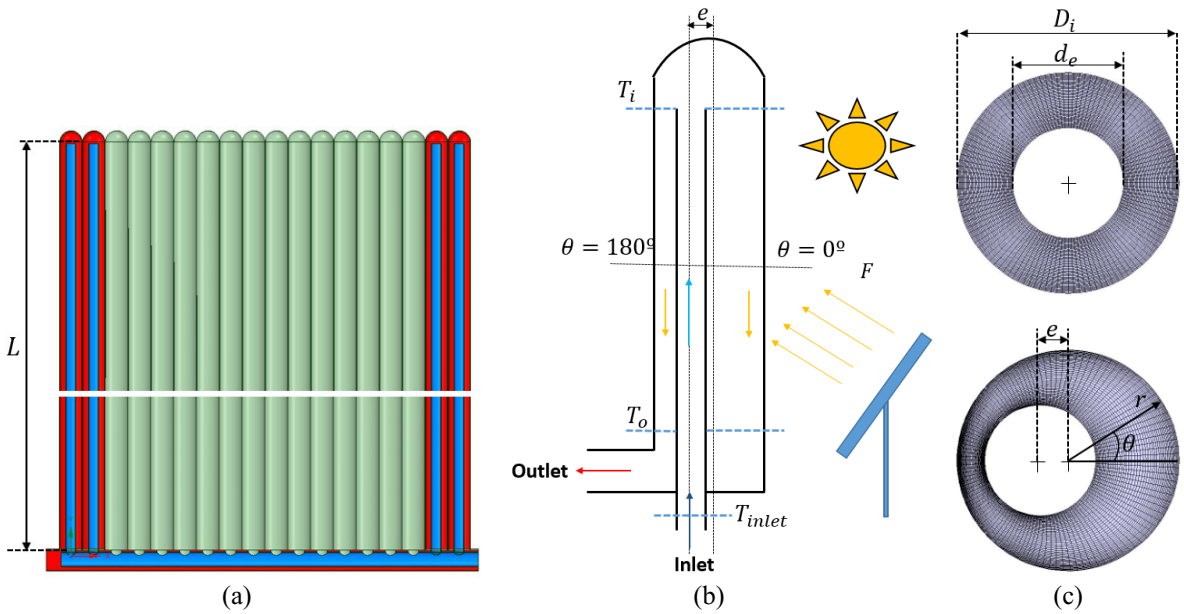

FIGURE 1. (a) Schematic representation of a receiver panel composed of bayonet tubes. (b) Section of a bayonet tube. (c) Computational mesh used in the CFD simulation.

CFD NUMERICAL SIMULATION

To study whether the bayonet tube, for the different working fluids analyzed and the same mean temperature, is able to reduce the risk of local overheating of the fluid and the tube, the simulation of fluid dynamics (CFD) will focus on the flow in the annular zone, Fig. 1 (c). The annular zone is the most complex one and is subjected to the highest temperature of the receiver. The commercial code *ANSYS Workbench v17.2* was used to create the geometry and mesh of the fluid field. The dimensions of the bayonet tube are 2.11 cm for the outside diameter of the inner tube, 4.46 cm for the outside diameter of the outer tube. The tubes have a thickness of 1.2 mm and a length of $L = 10\ m$. A fundamental aspect to consider is that the mesh must be thin enough near the walls of the outer tube to adequately capture the high thermal gradient that appears in this zone. After a sensitivity analysis it was observed that a mesh of the order of μm in radial direction is necessary to correctly describe the temperature gradient in the flow.

The CFD simulations of the velocity and temperature fields in the annular section of the bayonet tube, both in concentric and eccentric configurations, were carried out with the code *ANSYS Fluent v17.2* where the RANS equations of mass, moment and energy were solved in three dimensions. In addition, to properly capture the anisotropy of the turbulence [3], the seven turbulence equations of the RSM model (Reynold Stress Model) were solved too. All the equations were solved in a stationary state and with a second order precision in the convective and diffusive terms. The properties used in the simulation for molten salt, liquid sodium and sCO_2, taken from [4], [5] and [6] respectively, are temperature dependent. The molten salt is solar salt (60% $NaNO_3$ – 40% KNO_3). For the case of sCO_2 the pressure used to obtain the properties is $200\ bar$, which is a typical operation pressure in supercritical power cycles.

In this first study, for simplicity, the influence of the mechanical behavior (e.g. deformation and vibration) of outer and inner tubes onto the fluid has not been taken into account. The boundary conditions used in the simulations were obtained with the simplified model described in [7] for the most demanded panel (the fourth) of a bayonet tube receiver. Therefore, the temperature increase of the working fluids from the inlet to the outlet of the simulated tubes are only a fraction of the total temperature in the whole receiver. At the outlet of the annular section of the bayonet tube, the condition of *pressure-outlet* was imposed. All the walls were considered as non-slip surfaces. Since, according to the simplified model, the temperature in the inner tube of the bayonet tube does not present a high variation, it is not necessary to simulate the flow in the circular section of the inner tube in this first study. Instead, an average temperature of the flow in the inner tube, T_{inner}, and an overall heat transfer coefficient, U_{inner}, are used to couple the flow in the annular section of the tube with the flow in the inner tube. The overall heat transfer coefficient comprises the convection resistance of the flow in the circular section of the inner tube, the conduction resistance of this tube (INCOLOY alloy 800H $k_{tube} = 16.3\ W/mK$) and its fouling resistance ($R''_f = 8.85 \cdot 10^{-5}\ m^2K/W$). The same total increase in temperature (i.e. $T_o - T_{inlet} = 42.01\ K$) and total heat absorbed by the fluid between the inlet and outlet of the bayonet tube assembly were imposed in all the cases regardless the working fluid is with molten salt, liquid sodium or sCO_2. This leads to different working fluid velocities and mass flows. Table 1 summarizes the boundary conditions used in the simulation for the three working fluids analyzed.

TABLE 1. Boundary conditions used in the CFD simulations of the annular section of the bayonet tube.

Material	**Inlet**			**Outlet**	**Inner Wall**	
	Temperature T_i (K)	**Velocity $v_{z_{in}}$ (m/s)**	**Turbulence $k-\varepsilon$ (m^2/s^2)**	**Temperature T_o (K)**	**Heat transfer coefficient U_{inner} (W/m^2K)**	**Temperature T_{inner} (K)**
Molten Salt	**568.4**	**1.526**	**1 – 1**	**605.2**	**3482**	**565.8**
Liquid Sodium	**573.9**	**3.816**	**1 – 1**	**605.2**	**5264**	**568.5**
sCO2	**569.4**	**27.50**	**1 – 1**	**605.2**	**4110**	**566.3**

According to the simplified model [7], the heat flow absorbed by the outer tube is not uniform and depends on the angular position, θ. Thus, the flow of absorbed heat is maximum in the area of the receiver oriented to the field of heliostats, $\theta = 0^o$, while in the rear area of the tube, $|\theta| \geq 90^o$, only a residual, and almost uniform, heat flow is absorbed coming from the reradiating surface and the surrounding tubes. This distribution of the heat flux has been described in the simulation by a cosine function:

$$q''_s = \begin{cases} \left(q''_{s_{max}} - q''_{s_{rerad}}\right) \cdot \cos(\theta) + q''_{s_{rerad}} & if\ -90° \leq \theta \leq 90^o \\ q''_{s_{rerad}} & if\ 90° > \theta\ or\ \theta < -90° \end{cases} \quad (2)$$

Where $q''_{s_{max}} = 4.31 \cdot 10^5\ W/m^2$ is the maximum heat flow absorbed by the working fluid through the outer tube, per unit area in contact with the fluid, and $q''_{s_{rerad}}$ is the reradiating component that has been estimated to be 2.5% of $q''_{s_{max}}$ according to the simplified model.

RESULTS

In this section we present and analyze the results of CFD simulations of the annular section of the bayonet tube working with molten salt, liquid sodium and sCO_2. Firstly the hydrodynamic results will be studied, then the temperature of the fluid and finally the resulting heat transfer coefficient.

Hydrodynamic

Fig. 2 (a, b, c) shows a map of the axial velocity in the annular section of the bayonet tube at an intermediate axial distance from the entrance of the annular section, $z = 5\ m$. In this section the flow, which is turbulent in all the cases studied, see Table 2, is fully developed since z is much greater than the hydraulic diameter of the section. Fig. 2 also contains the radial profiles of axial velocity at $\theta = 0^o$. The velocity distribution is axisymmetric for the concentric case ($\xi = 0$), said symmetry not being broken by the variation of the properties with the temperature. The maximum axial velocity appears at an intermediate radius for all angular directions, θ. As the eccentricity grows, the axisymmetry is broken and a zone of maximum axial velocity located at $\theta = 0^o$ appears. This is so because at $\theta = 0^o$ the separation of the internal and external surfaces is maximized and the fluid is less affected by the friction of the fluid with the wall of the tube. Reciprocally, the minimum axial velocity is located at the rear region, $\theta = 180^o$, where the distance between the walls is minimal and therefore the influence of the walls is more noticeable.

TABLE 2. Average Prandtl and Reynolds numbers of the studied working fluids**.**

Material	Prandlt Number	Reynolds Number
Molten Salt	11.2	$2.042 \cdot 10^4$
Liquid Sodium	0.00554	$2.836 \cdot 10^6$
sCO_2	0.645	$3.599 \cdot 10^6$

In addition, viscosity plays an important role in axial velocity maps. For the working fluid with higher viscosity, i.e. the molten salt, the influence of the wall is more important, which implies a gradual decrease of the axial velocity in the vicinity of the walls (see Fig. 2). For the working fluid with less viscosity, i.e. liquid sodium, the area of maximum axial velocity is greater as the decrease of axial velocity is concentrated near the walls. It is important to note that, for the same mass flow in the annular section (viz. the same working fluid), the eccentricity increases the axial speed at $\theta = 0^o$. This increase of the velocity causes a greater dissipation of heat at $\theta = 0^o$, which is the most thermally demanded area. The same effect of the eccentricity on the hydrodynamic behavior of a flow was also observed in previous CFD simulations carried out with a LES turbulent model, [8]. Note that for all the different working fluids, when the eccentricity of the bayonet tube increases, there is a reduction in the pressure loss of the annular zone owing toa reduction of the coefficient of friction. This pressure loss, ΔP, is included in Fig. 2.

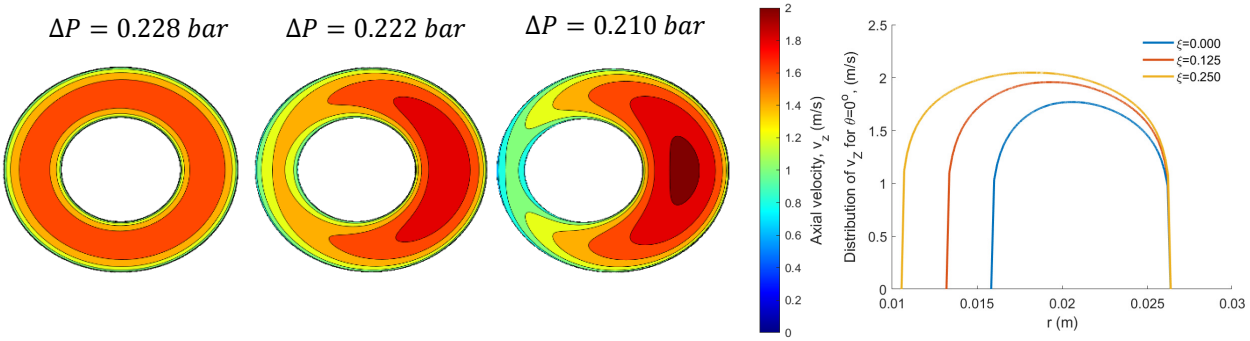

(a)

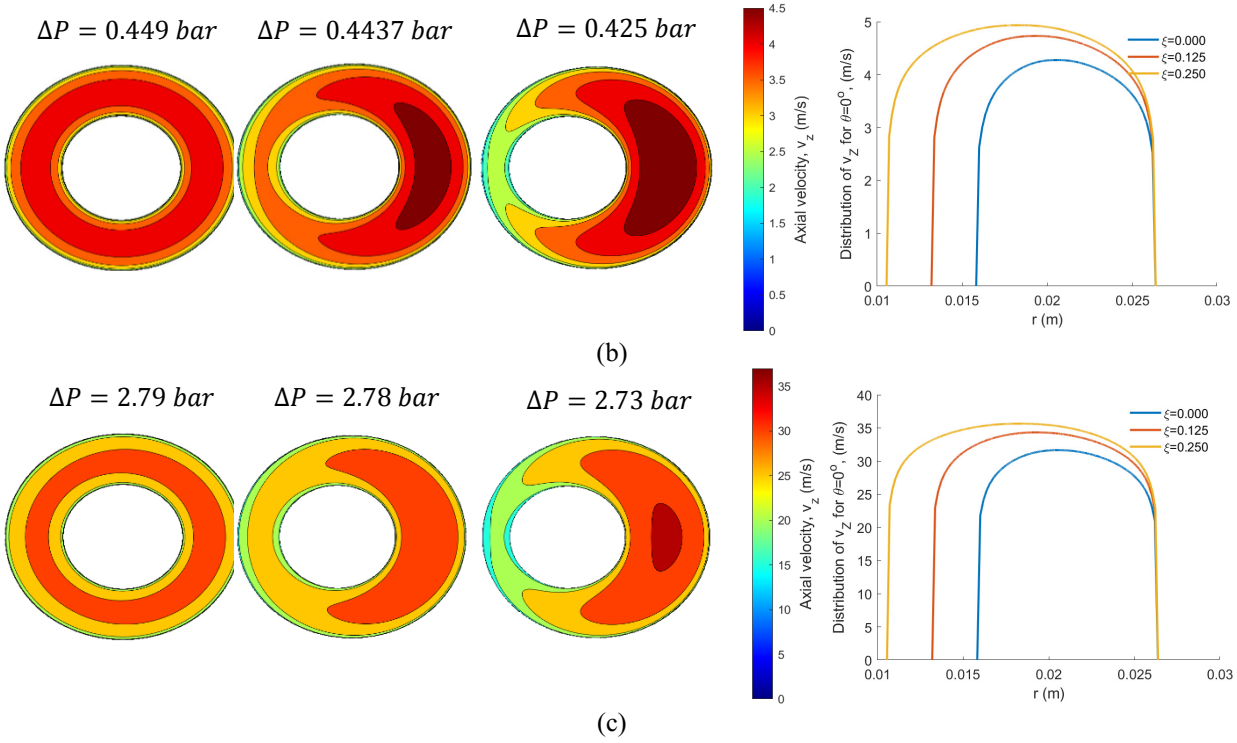

FIGURE 2. Maps and radial profiles of axial velocity at $z = 5\ m$ in the concentric ($\xi = 0$) and eccentric ($\xi = 0.125$ and $\xi = 0.250$) annular sections of the bayonet tube for: (a) Molten Salt, (b) Liquid Sodium and (c) sCO_2.

For molten salt, liquid sodium and sCO_2, the simulations also reveal the appearance of a secondary flow in the eccentric cases of the bayonet tube. The maximum secondary flow is located at angles around $\theta \approx 90^o$, as shown in the example of Fig. 3 (a) for liquid sodium. The recirculation of the flow is reflected in Fig. 3 (a) as a change of the sign in the horizontal component of the flow velocity, v_x. For the case of molten saltand for sCO_2, the simulation provides a behavior qualitatively similar to that shown in Fig. 3 (a) but with different magnitudes. However, the magnitude of these recirculation relative to the maximum velocity, $V_{X,max}/V_{Z,max}$, is quite similar for all the working fluids, see Fig. 3 (b), and grows with the eccentricity. In addition, the results of the secondary flow obtained here agree with those obtained in [8]. Therefore, these secondary flows that lead to better mixing of the fluid are due to the eccentricity and have nearly the same relative intensity for all the working fluids studied.

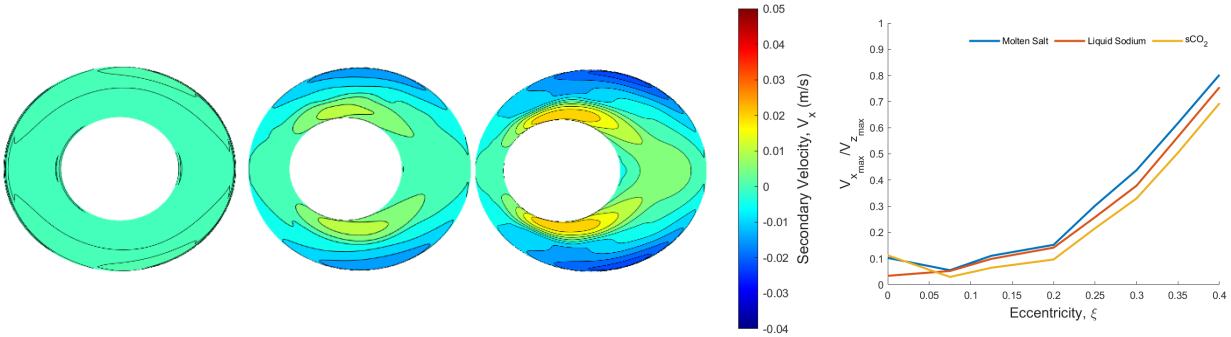

FIGURE 3. (a) Example of maps of secondary flow, v_X, at $z = 5\ m$ for the concentric ($\xi = 0$) and eccentric cases ($\xi = 0.125$ and $\xi = 0.250$) for liquid sodium. (b) Evolution of the ratio of the maximum horizontal velocity, $v_{X,max}$, and maximum axial velocity, $v_{Z,max}$, with the eccentricity at a height $z = 5\ m$.

Temperature of the Walls and the Working Fluid

In order to understand the behavior of the working fluid in the most thermally demanded zone, the radial distribution of the temperature for the different working fluids and different eccentricities has been represented in Fig. 4 (a, b and c) at $\theta = 0^o$. For the same eccentricity, if the conductivity of the working fluid is high, the hottest surface is better cooled, decreasing the temperature in said surface, and leading to a smoother thermal gradient, Fig. 4 (b). On the contrary, if the thermal conductivity is relatively small, the thermal gradient increases as well as the maximum temperature located of the flow. When the eccentricity is increased for a given working fluid, the surface temperature is also diminished, since the flow velocity at $\theta = 0^o$ is increased as seen previously, which enhances the cooling of the tube walls in that region of the annular section.

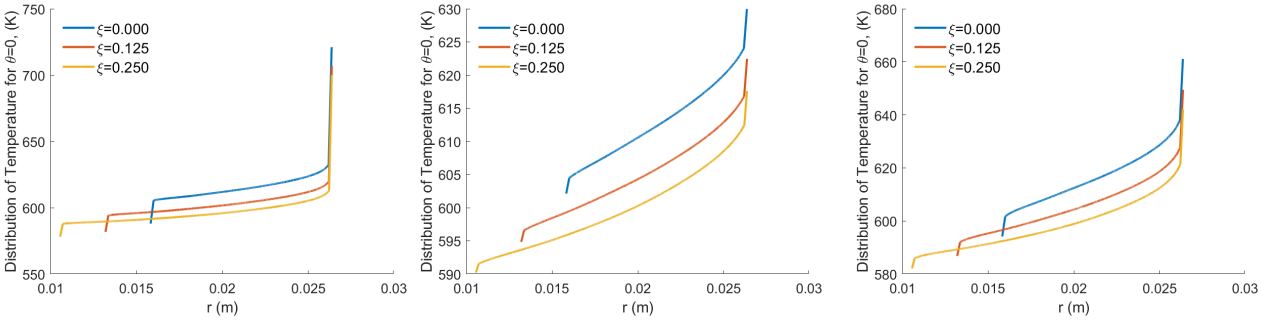

FIGURE 4. Radial temperature distribution at $\theta = 0°$ and $z = 5\ m$ for different eccentricities: (a) Molten salt, (b) Liquid sodium, (c) sCO_2.

Fig. 5 (a, b and c) shows the angular variation of the surface temperature at the inner surface of the outer tube obtained in the simulation for different eccentricities. This temperature is a critical variable, since it is equal to the highest temperature of the flow and also reflects how the flow is internally cooling the outer tube. As shown in Fig. 5, the temperature reaches a maximum at $\theta = 0°$ for the concentric configuration of the bayonet tube. Increasing the eccentricity causes a relative decrease of the temperature of the outer wall for $|\theta| < 90°$ because the velocity of the fluid increases in that region. This allows the fluid to transport more energy and better cool the walls of the tube. For $|\theta| > 90°$, these temperatures increase with the eccentricity due to the velocity reduction in this region, which also makes the temperatures more uniform than those for $|\theta| < 90°$. Since liquid sodium have a high thermal conductivity, the fluid temperature tends to be more homogeneous. Thus the angular variation and maximum temperature on the wall of the outer tube is less pronounced in the case of liquid sodium, Fig. (b), compared to the case of molten salt, Fig. (a). As the sCO_2 has an intermediate value of thermal conductivity, the angular temperature variation and the maximum temperature, Fig 5 (c) are between those of liquid sodium and molten salt.

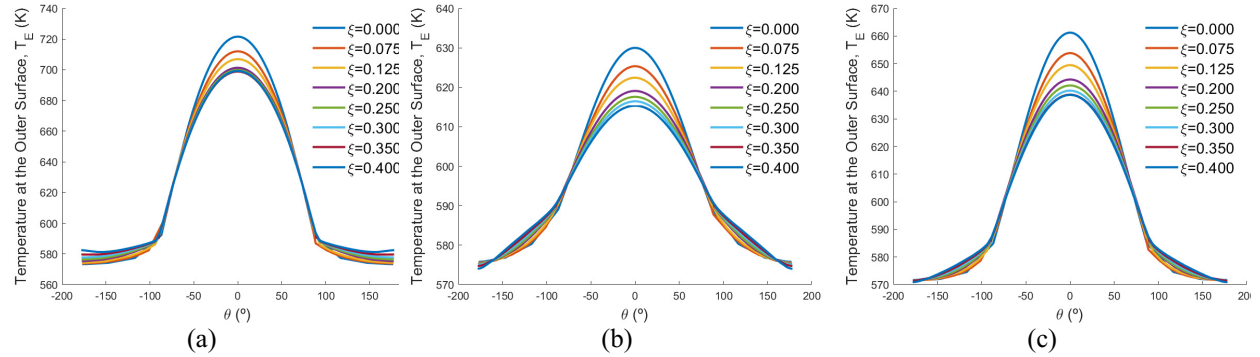

FIGURE 5. Temperatures at the inner surface of the outer tube at $z = 5\ m$ for different eccentricities (a) Molten salt, (b) Liquid sodium, (c) sCO_2.

Heat Transfer Coefficients

The usual definition of the heat transfer coefficient, h, uses the bulk temperature of the fluid in a given cross section. Due to the non-uniformity of the heat flux and the asymmetry of the annular section, this common definition leads to a negative convective coefficient in some areas of the bayonet tube, as was seen in [2]. This happens because the temperature of the contact surface in rear part of the outer tube can be lower than the bulk temperature of the flow. This fact indicates that the traditional definition of the heat transfer coefficient is not convenient in this case. For this reason, a new definition has been proposed in such a way that it considers the angular variations of the bulk temperature and heat fluxes.

$$h(\theta, z) = \frac{q_s''(\theta, z)}{T_s(\theta, z) - T_{m,\theta}(\theta, z)} \tag{3}$$

Where q_s'' is the heat flux dissipated by the wall surface, T_s is the temperature at the wall surface and $T_{m,\theta}$ is the radially averaged temperature, that can be called *angular bulk temperature*, which is the average of the fluid temperature, T, over a line at a constant θ in a section at constant z, weighted with the mass flux ($\rho \cdot v_z$) and the specific heat c_p of the working fluid:

$$T_{m,\theta}(z, \theta) = \frac{\int_{r_i}^{r_o} \rho \cdot v_z \cdot c_p \cdot T \cdot dr}{\int_{r_i}^{r_o} \rho \cdot v_z \cdot c_p \cdot dr} \tag{4}$$

Eq. 3 can be used to define the heat transfer coefficient of the outer surface of the annular section, h_E, if the temperature, T_s, and the heat flux, q_E'', of said surface are used. Fig. 6 (a, b and c) shows h_E as a function of the angular direction for a section at $z = 5\ m$ and different eccentricities. This section is representativeof what happens in the rest of the tube because the flow is turbulent flow and fully developed from about 20 cm from the inlet of the annular section inlet.

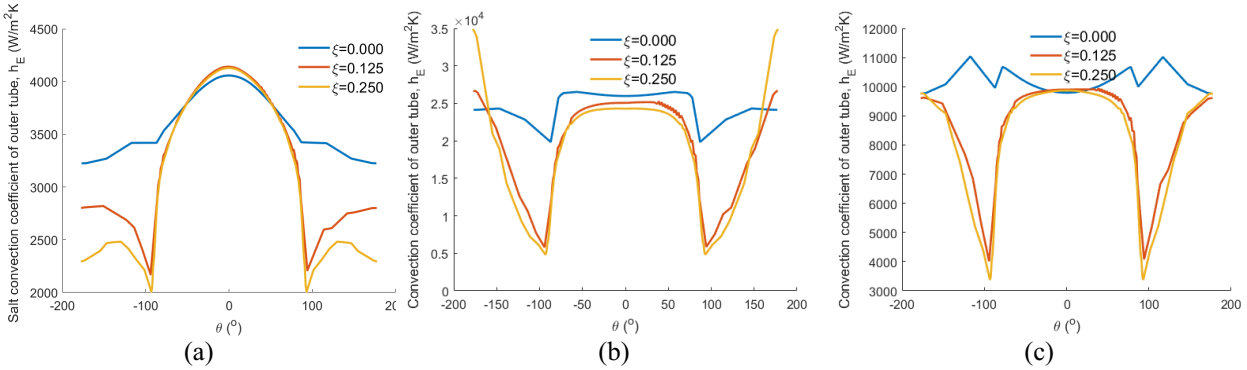

FIGURE 6. Angular variation of the coefficient of heat transfer for different eccentricities at $z = 5\ m$: (a) Molten salt, (b) Liquid sodium and (c) sCO_2.

With the new definition of Eq. (3), it can be seen in Fig. 6 that the convective coefficient is positive along all the angular directions, a fact that did not occur with the traditional definition, [2]. A non-uniformity of the convective coefficient is also observed, which differs from the uniformity typically assumed in the correlations for the turbulent convective coefficient. Regardless of the working fluid, the highest convective coefficient in the eccentric configurations appears at 0º, while lowest convective coefficient is located at $\theta = \pm 90^o$. Appreciable oscillations of the convective coefficient (e.g. sCO2 and ξ=0.25) are produced by the combined variation of both T_s and $T_{m,\theta}$ near $\pm 90^o$. There are very small oscillations of the convective coefficient around $\pm 60^o$ for ξ=0.125, which may be due to numerical instabilities accentuated when T_s approaches $T_{m,\theta}$ in Eq. 3. Besides, eccentricity does not seem to have a strong impact in the value of the convective coefficient in the frontal region, $|\theta| < 50^o$, with a slight increase for the case of the molten salt and a decrease for the cases of liquid sodium and sCO_2.

CONCLUSIONS

The CFD simulations shown in this paper indicate that eccentric bayonet tubes are advantageous over conventional tubes when used in receivers of solar power towers, where irradiation is extreme and highly non-uniform. The results show that, for liquid sodium, molten salt and sCO_2, the eccentricity slightly changes the convection coefficient on the surface of the outer wall in the frontal region, $\theta < 50°$. The eccentric bayonet tube improves the heat transfer coefficient 1.8% and 0.8% for molten salt and sCO_2, respectively and ξ=0.25, compared to the concentric bayonet tube. For liquid sodium, the convective coefficient decreases slightly with the eccentricity. Nevertheless, for molten salt, liquid sodium and sCO2, when passing from the concentric to the eccentric (ξ=0.4) configuration of the bayonet tube, the temperature of the hottest zone is reduced between 2.2% to 3%, which relieves the damage by thermal stresses on the walls of the tube and attenuates the degradation of the working fluid and the tubes of the receiver.

ACKNOWLEDGMENTS

The authors would like to thank the financial support provided by the Spanish government through the project ENE2015-69486-R (MINECO / FEDER, UE).

REFERENCES

1. Rodríguez-Sánchez M.R., Sánchez-Gonzalez A., Marugan-Cruz C., Santana D. (2014b). New Designs of Molten-salt Tubular-receiver for Solar Power Tower Plants, Energy Procedia 49, 504-513.
2. Pérez-Álvarez R., Rodríguez-Sánchez M.R., Acosta-Iborra A. and Santana-Santana D., Effect of eccentricity on the hydrodynamics and heat transfer of molten salt in bayonet receivers for solar power towers. Solar Power & Chemical Energy Systems Conference - SolarPACES 2017, September 26-29, Santiago de Chile.
3. Merzari E., Ninokata H. (2009). Anisotropic Turbulence and Coherent Structures in Eccentric Annular Channels, Flow Turbulence Combust 82, 93-120.
4. Zavoico A.B. (2001). Solar Power Tower: Design Basis Document, Sandia National Laboratories, 1-148.
5. Sobolev V. (2010). Database of thermophysical properties of liquid metal coolants for GEN-IV. SCK CEN, 1-175.
6. Colina C.M., Olivera-Fuentes C.G., Siperstein F.R., Lísal M., Gubbins K.E. (2003) Thermal Properties of Supercritical Carbon Dioxide by Monte Carlo Simulations, Molecular Simulation 29, 405-412.
7. Rodríguez-Sánchez M.R., Soria-Verdugo A., Almendros-Ibáñez J.A., Acosta-Iborra A., Santana D. (2014a). Thermal design guidelines of solar power towers, Appl. Therm. Eng. 428–438.
8. Nikitin N., Wang H., Chernyshenko S. (2009). Turbulent flow and heat transfer in eccentric annulus, J. Fluid Mech. 638, 95-116.